

Structural and Magnetic Properties of Electrodeposited CoPt and FeCu Nanowires Embedded in Polycarbonate Membranes

A. Kazadi Mukenga Bantu^{1,*}, A. C. de Castro², S. D. de Magalhães², V. M. T. S. Barthem², D. Givord³,
P. E. V. de Miranda⁴, G. Clemente⁴ and R. A. Simão⁴

¹*Physics Department, Faculty of Sciences, University of Kinshasa, Kinshasa 11,
Democratic Republic of Congo*

²*Instituto de Fisica/Depto de Fisica dos Solidos, Universidade Federal do Rio de Janeiro, Brazil*

³*Laboratoire Louis Néel, C.N.R.S., France*

⁴*Depto. Engenharia Metalurgica e de Materiais, COPPE, Universidade Federal do Rio de Janeiro, Brazil*

CoPt and FeCu multilayered nanowires arrays were successfully electrodeposited into nanochannels of commercial track-etched polycarbonate membranes. The deposited CoPt alloy had a face centered cubic structure and displays soft magnetic properties. The magnetic measurements had detected only ferromagnetic couplings between constituent layers of Co. Magnetic Force Microscopy measurements suggest that the Co magnetic moments are perpendicular to the wires axis and can rotate with respect to this axis in order to minimize the interaction of demagnetizing field. $\text{Fe}_x\text{Cu}_{1-x}$ alloys were prepared by electrochemical deposition from a sulfate bath of iron and copper ions. The composition of the alloys was obtained by the choice of the potential applied during the deposit. The obtained alloys crystallize in the fcc structure in accordance with the previous results. The first result obtained with FeCu nanowires denote a metastable phase for the system. The α -iron phase of stable bcc-structure at room temperature is ferromagnetic below its Curie temperature of 1043 K. Above $T=1193\text{K}$, γ -iron phase is stable in fcc-structure. However, it can be obtained in metastable state at room temperature using the necessary metallurgic procedures. Its magnetic properties depend on subtle elements not yet clearly understood that characterize its structural properties. Although, the iron and the copper are normally immiscible, Eckert et al. (1993) had shown that $\text{Fe}_x\text{Cu}_{1-x}$ alloys of fcc-structure can be prepared by "mechanical alloying". The obtained alloys are ferromagnetic for x values superior to 20. On the other hand, the fcc-structure alloys can also be prepared by electrochemical deposition (Uela and Kikuchi, 2004). But, in this case, no magnetic order was observed in the alloys. Therefore, they are paramagnetic whatever is the iron concentration.

1. Introduction

In the past few years, a significant attention has been paid to artificial magnetic nanowires because of their distinctive properties and potential uses for sensors and magnetic media. Synthesis and properties of arrays of magnetic nanostructures are of interest not only from fundamental but also from the technological point of view. Their main fundamental interest lies in the emergence of novel magnetic and transport properties as the dimension approaches the length scale of few nanometers to a few tens of nanometers [3]. Technological interest lies not only in the potential application to future high density data storage, electronics, optical devices, heat, and gas sensors, but also in their integration capabilities in functional micro and nanodevices (MEMS/NEMS). Recently, CoPt and

FeCu nanowires arrays were successfully electrodeposited into nanoporous alumina templates [4].

Electrodeposition of cobalt platinum and iron copper multilayers nanowires have been carried out using the single bath technique. The characteristics of these techniques are discussed briefly below.

The single bath [5] technique uses an electrolyte containing ions of both the constituents, and deposition is carried out by modulating either the plating current or the potential. In this method where we modulated the potential the concentration of ions of the nobler (more electropositive) metal in the electrolyte is much lower than the concentration of ions of the less noble metal. At a low current density (here at a low potential) only the nobler of the two metals is deposited, whereas at a high current density (here at a high potential) where the deposition of the less noble metal is diffusion limited an alloy rich in the less noble metal is obtained. The main limitations of this technique are

* albert.kazadi@unikin.ac.cd

the presence of most noble metal as impurities in the less noble metal deposit and the necessity of having metals with different deposition potentials. It was possible to limit the impurity concentration to 1% by minimizing the concentration of noble metal in the plating bath. In this case, a multilayer may be produced by switching the current density or the substrate potential between two values at which different metals are deposited. Since Pt (or Cu) is the more noble metal, it was present at low concentration in the electrolyte, and Co (or Fe) at high concentration. Pure Pt was deposited when the substrate potential was at 0.65 V, and an alloy consisting predominantly of Co when it was at 0.95 V. The same has been done for the FeCu multilayered Nanowires. Pure Cu was deposited when the substrate potential was at 0.25 V, and an alloy consisting predominantly of Fe when it was at 1.4 V.

The single bath technique has the obvious advantage that the substrate always remains immersed in the electrolyte limiting the risk of contamination. However, with this technique, the choice of the components of multilayers is limited. Moreover, the reduction potentials of the components must be sufficiently far apart to allow separate electrodeposition of each of components. Here, we report the electrodeposition of multilayered CoPt and FeCu nanowires in track etched commercial polycarbonate membranes. A very single bath of Co and Fe sulphate salts was respectively used for the Electrodeposition. The crystalline structure of multilayered nanowires was investigated by X-ray diffraction (XRD) with Cu-K_α radiation. The morphology has been characterized by SEM, AFM and MFM microscopy. And, the magnetic properties have been investigated by superconducting quantum device reference magnetometer.

2. Experimental Details

2.1. Electrolyte preparation

In this work, CoPt and FeCu multilayered nanowires were electrodeposited in commercial track-etched nanoporous polycarbonate membranes as shown in Fig. 1.

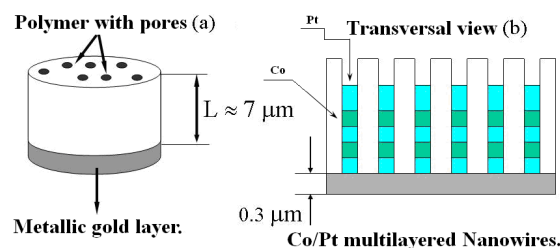


Fig.1: Schematic drawing of the membrane preparation and structure of the nanohole membrane: (a) conductive type (Au underlayer) (b) a penetration type of $\text{Co}_x\text{Pt}_{1-x}$ nanowire arrays in the supported nanoporous polycarbonate membrane.

We concentrated our work on these membranes made from thin foils irradiated with heavy ions and etched preferentially along the irradiation damage (see Fig. 5 and Table 1). Commercially available membranes can be purchased with nominal diameters values ranging from 10 nm to 500 nm [6]. All solutions were freshly prepared with water first doubly distilled and then treated with a Millipore Milli Q system. The electrolytes were composed of 14.2 mM $\text{CoSO}_4 \cdot 7\text{H}_2\text{O}$ and 0.142 mM K_2PtCl_6 for CoPt wires, and 14.2 mM $\text{FeSO}_4 \cdot 7\text{H}_2\text{O}$ and 0.142 mM $\text{CuSO}_4 \cdot 5\text{H}_2\text{O}$ for FeCu wires, respectively. The pH value of the electrolyte solution was about three (3). Boric acid 2.02g/l was used to facilitate the deposition procedure. Prior to immersion in electrolyte solution, the membranes have to be dipped in purified water under ultrasonic agitation for two minutes to ensure wetting of pores. A high concentration of Co in the electrolyte, as well as a large deposition current, is necessary to limit the amount of Cu co-deposited. Before and during the electrodeposition, solutions were de-aerated with argon to reduce the amount of dissolved oxygen in order to avoid oxygen incorporation into materials during the electro-deposition process, which was performed at 25°C.

2.2. Electrochemical cell and instruments

Electro-deposition has been carried out potentiostatically at room temperature in a three conventional electrodes cell connected to a Potentiostat GP 201 H (home made Galvpot GP 201 H/COPPE/UFRJ). A thin layer of gold was then sputter deposited onto one side of the templates in order to serve as a cathode (working electrode WE). All potentials of the working electrode were measured with respect to a saturated calomel electrode (SCE) reference. The counter electrode (CE) was a platinum spiral used as shown

in Fig. 2. In this figure, we could observe how three electrodes, WE, SCE, and CE, were connected to the Galvpot 201. The iron and copper compositions were analyzed by x-ray fluorescence analysis (XRF) for FeCu wires. We did not make this for CoPt wires.

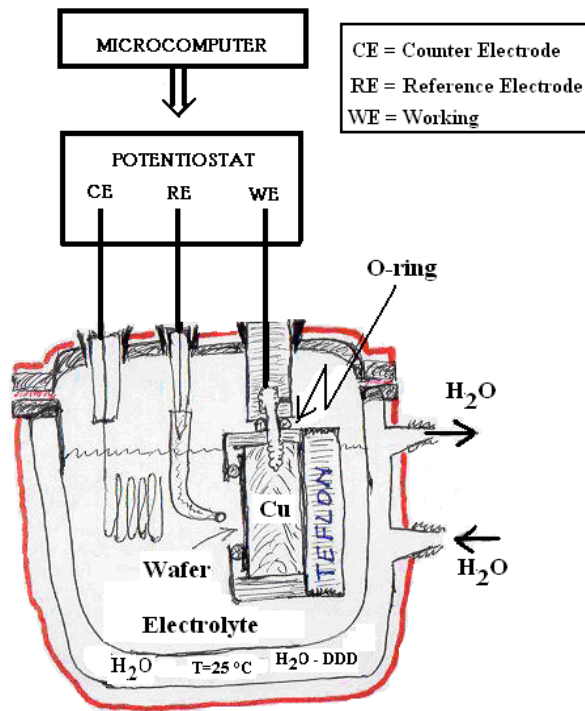


Fig.2: Cross-section of electrochemical cell, and schematic illustration of the electrodes arrangement for fabrication of electrodeposited CoPt and FeCu multilayered nanowires.

The growth morphology and alloying composition of the as-deposited multilayered nanowires have been characterized using an x-ray fluorescence analysis (XRF). The scanning electron microscopy (SEM), as well as the atomic force microscopy (AFM), was employed for examining the coverage and the uniformity of the deposit. Magnetic property measurements were performed at room temperature using a superconducting quantum interference device (SQUID) magnetometer.

3. Theoretical considerations

3.1. Estimation of layer thickness

Pulse potential deposition technique using single bath is basically defined in terms of the potential variations with time corresponding to desired layer thickness. The membrane thickness divided by the total number of cycles required for filling of the pores gives the bilayer thickness. In order to obtain a uniform layer thickness along the whole nanowires we used a method that is based on relation between the layer thickness of each component and the electrical charge transferred during the pulsation potential. Each cathode potential is set by a computer-controlled potentiostat that numerically integrates the current and monitors the electric charge that passes during each time interval. Below we set out to obtain a linear relation between the bilayer thicknesses with respect to the variation of Pt charge and to calculate the current efficiency for Co deposition when using the pulse potential technique. The intention is to demonstrate an improvement in uniform bilayer thickness along the nanowires by controlling the bilayer thickness through the electrical charge passed during each pulse. Based on Faraday's law, the amount of deposited Co and Pt can be calculated by the formula

$$m_i = \frac{M_i Q_i}{n_i F} \cdot \eta_i \tag{1}$$

Where, m_i is the weight of deposited metal ($i = \text{Co}, \text{Pt}, \text{Fe}, \text{Cu}$), M_i the molecular weight, n_i is the number of charge passed during the deposition process, F is the Faraday constant, Q_i is transition charge corresponding to desired layer thickness, and η_i is the current efficiency. Additionally, the amount of deposited films m_i can be expressed in terms of current density as

$$\rho * A * d_i = m_i \tag{2}$$

Where, A is the cathode surface area, which depends on the pore density and the diameter of membrane, d_i is the thickness of the deposited layer. By placing Eqn. (2) into Eqn. (1) the layer thickness of Co as well as Pt, Fe, and Cu can be determined.

Since the periodic multilayers of Pt and Co are formed by sequentially growth of these two layers, the modulation wavelength ($d_{bilayers_i}$) can

conclusively be defined as the sum of the layers thickness, d_{Co} and d_{Pt} .

3.2. Identification of the pore-filling process

The wire growth by a complete pore-filling process was studied with chronoamperometry (I-t characteristics curve) experiments. The current response during reduction of Co ions at constant applied potential of -8.5 V is shown in Fig. 3. Since the deposition current depends on mass transport conditions and effective surface area of the electrode, the recorded I-t curve during Co deposition revealed four different stages [7]: (I) initially, the current decreases due to mass transport limitation; (II) the metal is growing into the pores and a slightly increasing current is observed as the distance to the pore opening becomes smaller until; (III) the pores are filled to the top of membrane surface and give rise to a cap formation associated with three dimensional deposition; and consequently (IV) the hemispherical caps originating from each nanowires form a coherent planar layer that expended to cover the whole surface of the membrane.

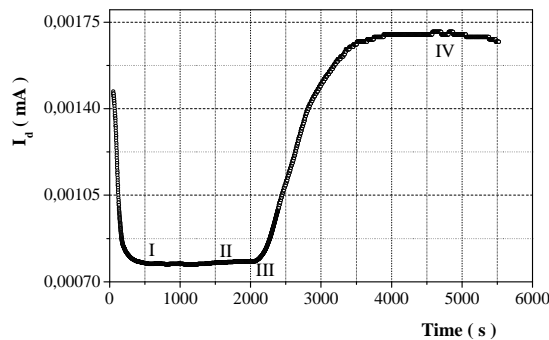


Fig.3: The different stages of pore filling process during cobalt deposition at - 8.5 V. The first complete filled pores can be indicated when a rapidly increasing current is observed. Electrochemical reduction current (I) is given as function of time (t) for potentiostatic deposition of cobalt. In part (I) metals are starting to grow into the wires. Part (II) the pores are completely filled. Part (III) three dimension hemispherical caps are obtained. Part (IV) the metals are grown over the wires and cover a membrane.

Thus, the effective cathode area increases and a rapidly increasing deposition current can be observed. For the present application, the electrodeposition process was stopped at stage (II), before filling completely the membrane.

4. Results and Discussion

Fig. 4 shows voltammograms recorded in the electrolyte containing both Co and Pt ions. From this curve, it is seen that a Pt deposition peak is observed with a maximum slightly below 600 mV. This is followed by a minimum in the current density approximately 900 mV, which after Co deposition becomes the dominating process.

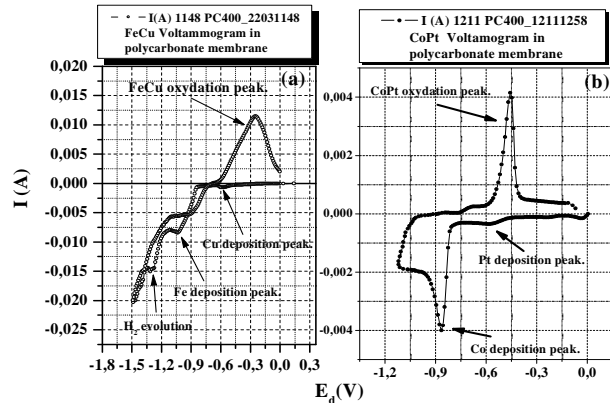


Fig.4: Current–voltage characteristics corresponding to deposition of (a) (left) the Fe and Cu, and (b) (right) Co and Pt from an aqueous electrolyte of 1 mM Cu_2SO_4 or K_2PtCl_6 and 100 mM and $FeSO_4$ or $CoSO_4$, respectively.

Notice that no hydrogen reduction as a parallel reaction to Pt deposition is observed at low potentials. This indicates that Pt is deposited with a current efficiency of 100% in the potential range from 200 to 1000 mV.

In this figure, we can observe the voltammogram recorded in the electrolyte containing both Fe and Cu ions. As for the electrolyte containing both Co and Pt ions, one could see that Fe and Cu deposition peaks are observed approximately below 600 mV for Cu and slightly up 1000 mV for Fe. We observed that it was difficult to conduct deposition because of the hydrogen evolution at - 1.3 V as shown in Figs. 4(a) and 5.

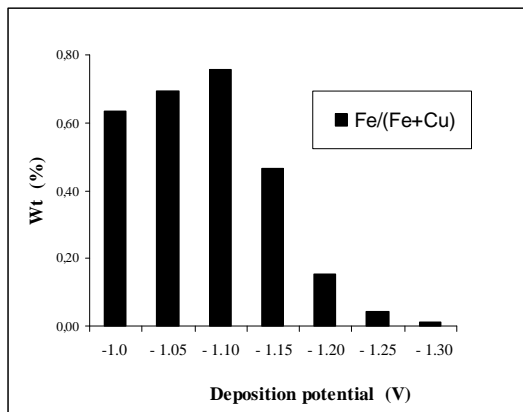


Fig.5: Composition of Fe and Cu in different electrodeposited samples from (XRF) modulating the applied potential.

This phenomenon makes difficult the depositions of FeCu multilayered nanowires as we could observe it in Fig. 5. The good deposition reached to 1.10 V.

Fig. 6 shows the typical pulse potential and current-time transient set up for Co/Pt multilayered nanowires deposition measured during the deposition of these nanowires. The high negative currents correspond to deposition of Co at - 0.95 V, while the low currents correspond to deposition of Pt at - 0.65 V. Note that when the deposition potential is switched from - 0.95 to - 0.65 V the current is always negative (cathodic).

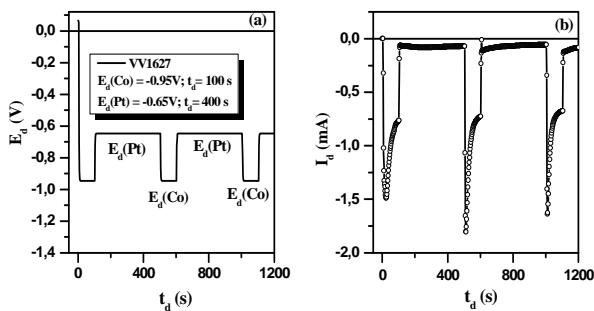


Fig.6: Part of an experimental modulation curves used (a) potential and (b) current transient, recorded during the electrodeposition of a CoPt alloy formed by the alternate deposition of Pt and Co. A negative current indicates metal deposition.

This is an indication that we did not have dissolution of the less noble metal or, e.g., double layer discharge. We have well chosen our deposition potentials.

4.1. Morphology and structural properties

In this study, commercial track-etched nanoporous polycarbonate membranes were used to grow the CoPt / FeCu multilayers wires arrays. Fig. 7 shows a SEM image top-view of commercial track-etched nanoporous polycarbonate membrane with a pore diameter of 400 nm.

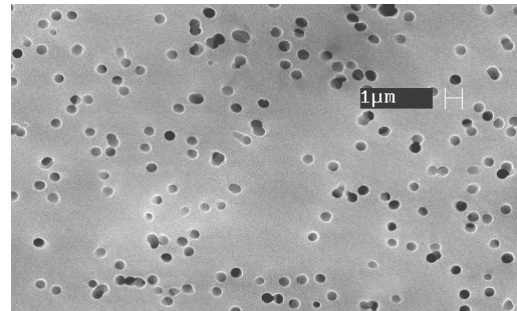


Fig.7: Top view SEM image of commercial etched track polycarbonate membrane with pore diameter of 400 nm.

One could observe that the pores are randomly distributed. Fig. 8 illustrates the SEM micrographs of CoPt nanowires grown in porous membranes after dissolution of the membrane in dichloromethane (Cl₂CH₂). The wire width was the same as the pore diameter; 400 nm. Table 1 shows the specification of PC membrane used in the present work.

Table 1: Specification of PC membrane used in all experiments.

Parameter	Value
Pore diameter [nm]	400
Membrane thickness [μm]	7
Pore density [pores/cm ²]	2x10 ⁶

The structural properties of CoPt and FeCu multilayered nanowires arrays have been investigated by X-ray diffraction at Cu-K_α wave length (λ=1.5405Å). The XRD diagrams are presented in Fig. 9. The as-deposited Co_xPt_{1-x} nanowires shows an fcc structure with a preferred (200) growth orientation. Only the (111), (200), (110), and (112) peaks are observed. They correspond to CoPt multilayered nanowires with fcc texture. These patterns reveal that both the CoPt and FeCu are polycrystalline with a weak (111) texture.

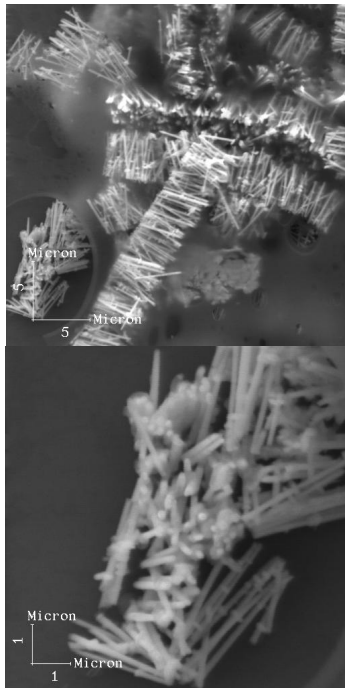


Fig.8: SEM image of 400 nm in diameter and ~ 4µm long deposited nanowires. CoPt nanowires are produced at $E_d(\text{Co}) = -950$ mV and $E_d(\text{Pt}) = -650$ mV.

In multilayers two mechanisms contribute to favour the FCC phase: on one hand, the presence of Pt or Cu impurities, on the other hand, the presence of Co/Pt or Fe/Cu interfaces, since Pt or Cu is always FCC and the lattice mismatch of the two metals favours a FCC Co or Fe phase.

4.2. Determination of the composition of the FeCu alloys

Because of different conductivities and reduction potentials of iron and copper their rate of deposition from a common bath will be different. Because of this the final composition of the material deposited could be quite different from that taken in the bath. We measured the final composition using X-rays fluorescence (XRF). Ratio of the area under the peak of Fe ($K\alpha+K\beta$) and Cu ($K\alpha+K\beta$) in the XRF spectrum is used to obtain the relative atomic concentration in the iron–copper alloys. Fig. 10 shows the energies of X-rays for several elements versus the channel number in the multi-channel analyzer (MCA) that was used for the energy dispersive data acquisition. The straight-line behavior ensures the linearity of the system.

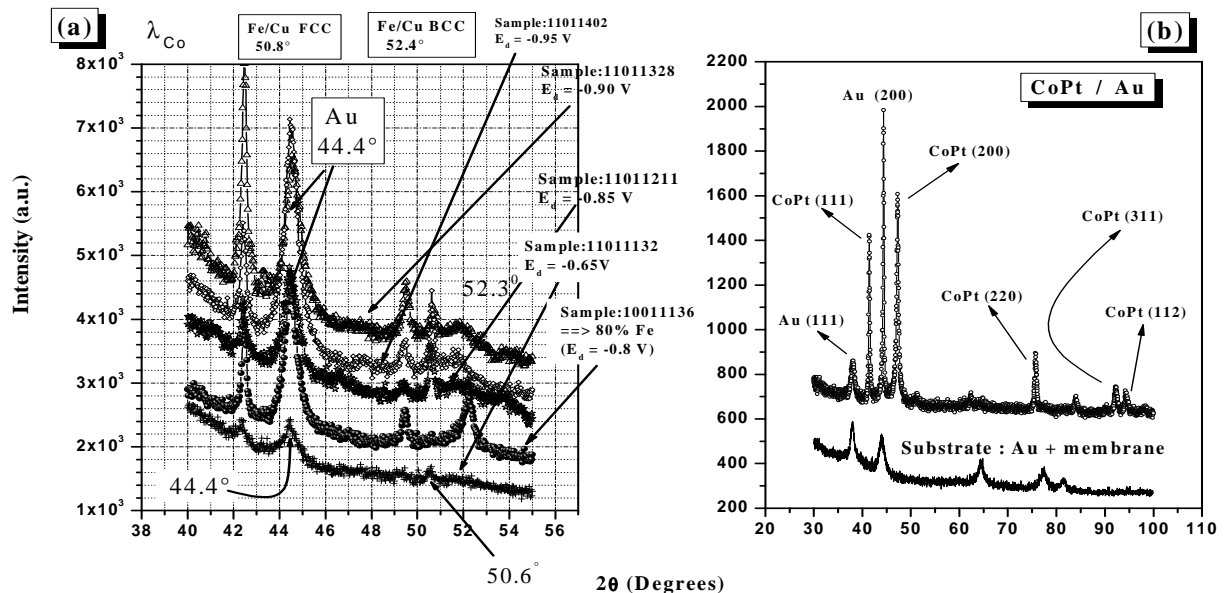


Fig.9: XRD shows an fcc structure corresponding to the disordered phase of the (a) $\text{Fe}_x\text{Cu}_{1-x}$ and (b) $\text{Co}_x\text{Pt}_{1-x}$ wires.

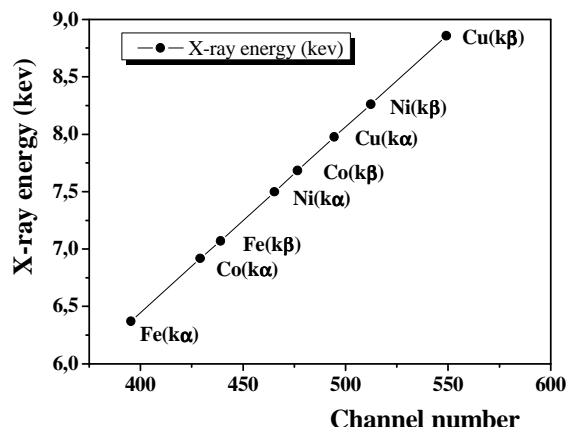


Fig.10: X-ray energy versus channel number.

Important point here is that Fe and Cu peaks are well separated so that in the case of alloy or mixture of these two constituent elements, one can calculate the area under the Fe peaks ($K\alpha+K\beta$) and Cu peaks ($K\alpha+K\beta$) quite accurately. The XRF setup was calibrated for the Fe–Cu system by measuring areas under Cu and Fe peaks for five different mixtures of Fe and Cu compounds in known proportion.

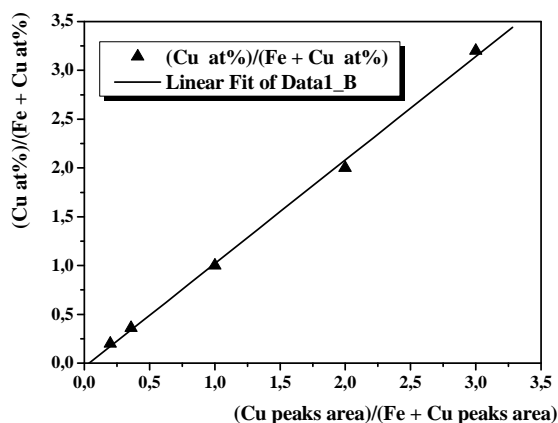


Fig.11: Plot of $(\text{Cu at\%})/(\text{Fe} + \text{Cu at\%})$ from the known composition versus the ratio $(\text{Cu peaks area})/(\text{Fe} + \text{Cu peaks area})$ from XRF.

Fig. 11 shows the plot of $(\text{Cu at\%})/(\text{Fe} + \text{Cu at\%})$ from the known composition versus the ratio $(\text{area under Cu peaks})/(\text{area under Fe} + \text{Cu peaks})$ in the corresponding XRF spectrum. This straight-line plot was used as calibration to find Cu/Fe composition in the alloys made in this work. In fact, the area ratio is almost the same as the ratio of their atomic concentrations.

In order to investigate the composition of nanowires corresponding to cathodic potentials observed in Figs. 4, experiments at constant potentials of -1.2 ; -1.05 ; -0.89 ; -0.85 ; -0.83 ; -0.8 ; -0.6 ; and -0.5 V (vs. SCE) were performed. Consequently, the concentrations of Fe and Cu in the respective nanowires layer determined by XRF as a function of cathodic potentials can be found in Fig. 12. The layers deposited at -1.2 V (vs SCE) are composed of 97 wt.% Fe and 3 wt.% Cu . Cu nanowires deposited at -0.5 V is 100% pure. These results are in accordance with the voltammetric behavior presented in Fig. 4b.

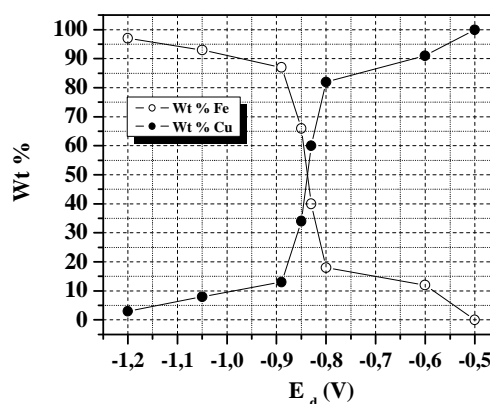


Fig.12: Chemical composition of deposited materials in porous polycarbonate membrane.100 wt % Cu is deposited at potential, $E_{(d)} \approx -0.5$ V while at $E_{(d)} = -1.2$ V the deposits comprise of 97 wt % Co and 3 wt % Cu.

Fig. 13 shows the XRF spectrum for the alloy ($x = 68$ at% Fe) sample recorded under the same experimental conditions. The XRF analysis of the nanowire arrays in this figure shows that Fe and Cu were the main elemental components.

For all the alloys the peak positions are the same but the areas are different. From these studies, we find that the value of x for our samples $\text{Fe}_x\text{Cu}_{100-x}$ are $x = 97, 93, 87, 66, 40, 18, 11, 0$ wt%, respectively.

Fig. 14 shows a histogram of a series of samples synthesized at different potentials. One could see how the amount of Fe increases and the amount of Cu decreases with an increase in applied potential, respectively. The X axis represents the samples as prepared decreasing the applied potential, and the Y axis represents the counts (a.u.).

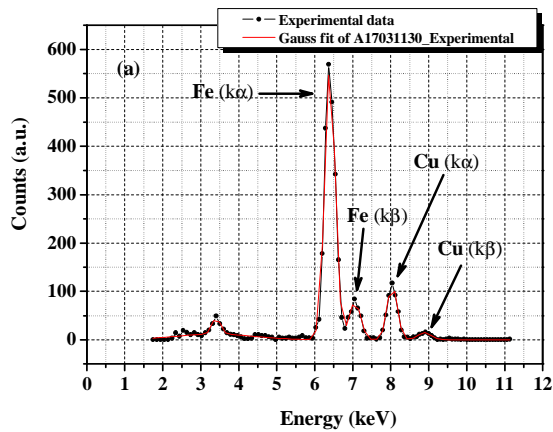


Fig.13: The XRF analysis of the $Fe_{68}Cu_{32}$ alloy nanowires recorded under the same experimental conditions.

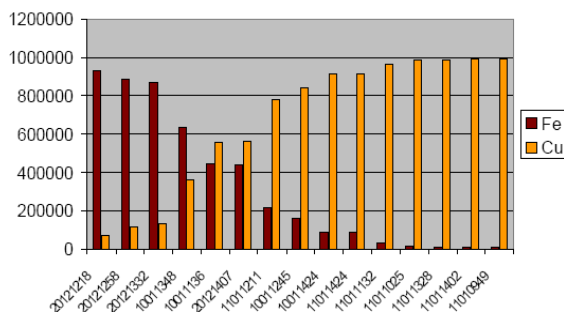


Fig.14: Composition of Fe and Cu in different electrodeposited samples from (XRF) modulating the applied potential.

4.3. Magnetic properties

Magnetic properties were investigated at 300 and 10K for the as-deposited samples. Typical hysteresis loops, measured at 300K for the as-deposited CoPt and FeCu samples are shown in Figs. 15 and 16, respectively. For these two samples, a hard magnetic behavior is observed and the easy axis of magnetization is parallel to the wires. As can be seen in Fig. 15(a,b), magnetic measurements had detected only the ferromagnetic coupling between constituent layers of Co. This magnetic behavior is similar to that observed in molecular beam epitaxy (MBE) grown Fe/Cu (001) films from which it is known that evaporated Fe on Cu (001) at room temperature shows a fcc/bcc phase transition. The presence of fcc Fe can be explained by the fact that the rapid growth of these nanowires causes considerable tensile stress [8].

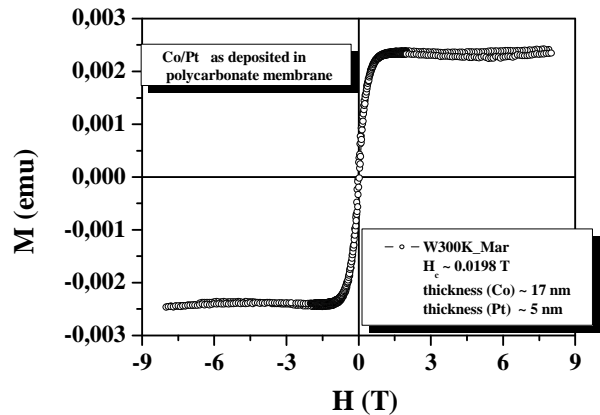


Fig.15(a): Hysteresis loop of CoPt wires measured at room temperature with magnetic field parallel to the wires axis.

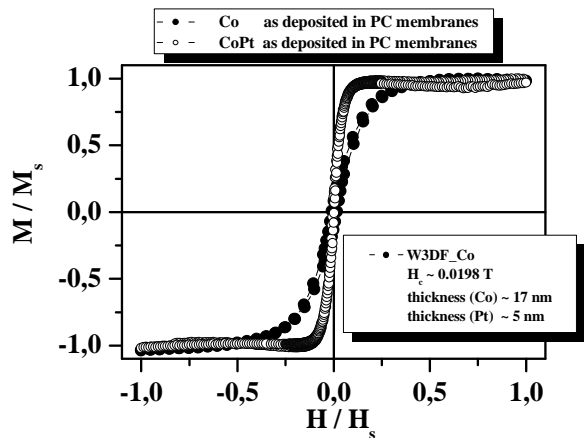


Fig.15(b): Hysteresis loop of Co and CoPt wires measured at room temperature with magnetic field parallel to the wires axis.

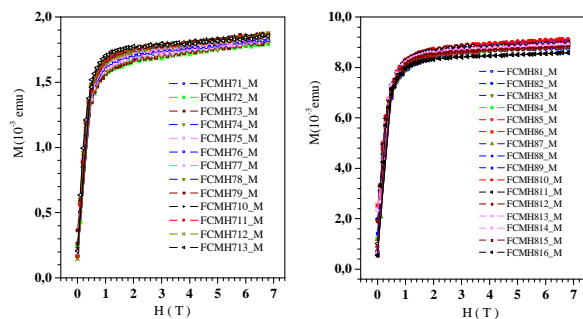


Fig.16: Hysteresis loops for two FeCu samples annealed at different temperatures.

After CoPt alloy wires have been electrodeposited into the membranes, the structural and magnetic measurement characterizations have been conducted by AFM and MFM microscopy on CoPt wires after they have been liberated from the polycarbonate membranes in dichloromethane (Cl_2CH_2). Fig. 17 shows (a) an atomic force microscopy (AFM) image of the sample with very good uniformity and top flatness of CoPt wire for which the average length is about $2.8 \mu\text{m}$; and its corresponding (b) magnetic force microscopy image (MFM) with wire magnetized alternatively up (white) and down (black). They both reveal sharply defined structures and wire uniformity over a large area. The MFM measurements for the same sample suggest that the magnetic Co moments are parallel to the axis of wires and can turn with respect to the axis in order to minimize the interactions of demagnetizing field.

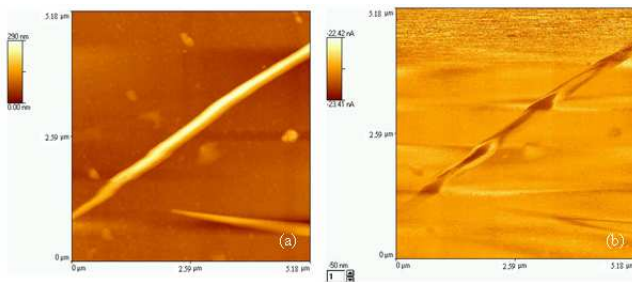


Fig.17: (a) AFM image of the sample showing very good uniformity and top flatness of CoPt wire for which the average length is about $2.8 \mu\text{m}$; and its corresponding (b) magnetic force microscopy image (MFM) showing wire magnetized alternatively up (white) and down (black). They both reveal sharply defined structures and wire uniformity over a large area.

Non-equilibrium techniques such as ball milling [4–7], co-vapor deposition [8], rapid quenching, RF sputtering, ion-beam mixing, etc. have been used to prepare $\text{Fe}_x\text{Cu}_{100-x}$ and $\text{Co}_x\text{Pt}_{100-x}$ meta-stable alloys at almost all compositions. High iron concentration leads to a BCC phase and a low iron concentration to an FCC phase. There is a range in between for which mixed BCC and FCC phases occur. The range of compositions forming BCC or FCC metastable alloy is found to be highly dependent on the preparation method. For ball-milled Fe–Cu alloys, the structure is BCC for iron between 75% and 100%, whereas it is FCC for 0–60% iron. Mixed BCC and FCC phases appear for iron 60–75%. Alloys made by rapid thermal quenching show mixed phase for 19–85% iron concentration. Mixed BCC and FCC phases occur at 40–55% iron for films made by sputtering, at

35–60% for thermally evaporated films and at 27–30% for the electrodeposited films. In the FCC phase, the alloy is found to be paramagnetic, whereas in the BCC phase it shows magnetization smaller than what can be expected from a simple dilution law.

As can be seen from Figs. 15 and 16, all loops exhibit a square shape due to a strong perpendicular anisotropy. Therefore, from these results one can infer that the Co/Pt or Fe/Cu wires show a significantly different behaviour with a squared hysteresis.

5. Conclusion

We achieved the electrodeposition of CoPt and FeCu multilayered nanowires into polycarbonate membrane substrate where Pt and Cu are noble metals. The objective of this study was to investigate the coupling mechanisms that oscillate in a system of confined geometry. We describe here the method of preparation for electrolytic deposit and the first magnetic characterizations. The magnetic measurements from SQUID had detected only ferromagnetic couplings between constituent layers of Co. MFM measurements suggest that the magnetic Co moments are perpendicular to the wires axis and can rotate with respect to this axis in order to minimize the interaction of demagnetizing field. We were thus able to produce nanowires in which Fe or Co was dominated by the FCC phase. Magnetic measurements performed on arrays of wires showed that the FCC phase is necessary to ensure a large squareness of the hysteresis curve. However, it appears that their presence in larger concentrations (when compared to those in pure electrodeposited metals) plays a key role in stabilizing metastable electrodeposited alloys out of immiscible components, like Fe, and Cu.

Acknowledgements

The authors are grateful to the Fundação Carlos Chagas Filho de Amparo a Pesquisa do Estado do Rio de Janeiro (FAPERJ) for their financial support through the project N^o: E-26/151.031/2002.

References

- [1] J. Eckert, J. C. Holzer and W. Johnson, *J. Appl. Phys.* **73**, 131 (1993).
- [2] Y. Ueda and N. Kikuchi, *Jpn. J. Appl. Phys.* **32**, 1779 (1993);
M. K. Roy, V. S. Subrahmanyam and H. C. Verma, *Phys. Lett. A* **328**, 375 (2004).

- [3] M. Almane et al., J. Phys. D: Appl. Phys. **39**, 4523 (2006).
- [4] Y. Dahmane et al., J. Phys. D: Appl. Phys. **39**, 4130 (2006).
- [5] U. Cohen, F. B. Koch and R. Sard, J. Electrochem. Soc. **130**, 19838 (1987);
I. Kazeminezhad et al., Appl. Phys. Lett. **78**, No.7, 1014 (2001);
M. Chen et al., Appl. Phys. Lett. **82**, No.19, 3310 (2003).
- [6] Millipore - Isopore® Membrane Filters;
Poretics Corp., 111 Lindbergh Av.,
Livermore, CA 94550-9520;
Costar Corp. (Nuclepore), One Alewife
Center, Cambridge MA 02140;
Whatman SA, 1 lb Av. Einstein, B-1348
Louvain-la-Neuve, Belgium.
- [7] A. Kazadi Mukenga Bantu et al., J. Appl. Phys. **89**(6), 3393 (2001).
- [8] K. G. Budinsky, *Surface Engineering for Wear Resistance* (Prentice-Hall, Englewood Cliffs, NJ, 1988);
J. R. Roos, J.-P. Celis and M. De Bonte, in:
R. W. Cahn, P. Haasen, E. J. Kramer (Eds.),
Materials Science and Technology, Vol.15,
VCH (1991) p.481.

Received: 21 October, 2014

Accepted: 13 February, 2015